International Journal of GEOMATE, March, 2026 Vol.30, Issue 139, pp.126-135
ISSN: 2186-2982 (P), 2186-2990 (O), Japan, DOI: https://doi.org/10.21660/2026.139.g15303
Geotechnique, Construction Materials and Environment

EVALUATION OF SEASONAL IMPACTS OF RIVER INFLOW ON PHYSICAL FIELDS IN HARIMA NADA BY USING OCEAN MODEL

* Nar Wuriga[1], Valentina Pintos Andreoli[2], Motoharu Suzuki[3], Yutaro Koga[3], Tomohito Matsuo[1] and Hikari Shimadera[1]

[1]Graduate School of Engineering, The University of Osaka, Osaka, Japan; [2]Port and Airport Research Institute, Kanagawa, Japan; [3]Hyogo Prefectural Institute of Environmental Sciences, Hyogo, Japan

*Corresponding Author, Received: 30 May 2025, Revised: 30 Dec. 2025, Accepted: 02 Jan. 2026

ABSTRACT: Over the past three decades, oligotrophication in Harima Nada, Japan, has caused ecological and fisheries impacts, leading to the implementation of nutrient management in coastal waters. As a semi-enclosed sea with limited exchange with the open ocean, its hydrodynamics are influenced by river inflow and atmospheric conditions. In this study, we investigated the seasonal impacts of river discharge on the physical fields of Harima Nada using a model system that coupled the Regional Ocean Modeling System (ROMS) with the Weather Research and Forecasting (WRF) Model by comparing simulations with and without river inflow. Including river inflow improves the reproducibility of seawater temperature and salinity across the basin, reducing the annual RMSE by 0.13 °C and 1.59 PSU, respectively. As a combined effect of temperature and salinity, water column stability reflects the seasonal influence of freshwater input, with stratification strengthening under high discharge and weakening under low discharge. Freshwater source analysis indicates that the Yodo River and the Kako River are the dominant contributors, with seasonal mean fractions of 22% and 16%, respectively. Overall, river discharge influences density stratification throughout the entire water column, suppressing vertical mixing and improving model performance. When stratification is weak, the influence of river input throughout the water column is correspondingly reduced. The results offer practical guidance on managing treated effluent and implementing coastal monitoring strategies.

Keywords: Stratification, Seasonality, River inflow, Oceanographic simulation, Harima Nada

1. INTRODUCTION

During the period of rapid economic growth in the 1960s, Harima Nada, located in the eastern part of the Seto Inland Sea, Japan, experienced significant eutrophication due to increased industrial activity and wastewater discharge. However, in the following decades, strengthened environmental regulations and sustained reductions in nutrient inputs gradually shifted these waters toward a more oligotrophic state. Although nutrient concentrations in the seawater have decreased over time, the continued decline in nutrient levels has reduced marine productivity and negatively affected the fisheries industry [1-3]. Consequently, the question of how to manage nutrient levels effectively, balancing ecological conservation with fishery sustainability, has gained growing attention in recent policy discussions [4]. As part of recent management initiatives, the deliberate introduction of nutrients through treated sewage effluent has been increasingly advocated in Harima Nada. This measure is intended to mitigate the progressive decline in nutrient concentrations. Previous extensive observational and modeling studies have been conducted in the Seto Inland Sea and Harima Nada [4-9] to investigate its circulation characteristics, water quality, and environmental variability. These studies have employed a variety of numerical models and monitoring approaches to describe the physical and biochemical features of the region. Most ocean dynamic modeling studies focusing on Harima Nada have relied on offline atmospheric forcing, in which atmospheric variables are prescribed from reanalysis products, pre-calculated atmospheric simulations, or observational time series. Reanalysis datasets are widely used as atmospheric forcing in ocean simulations; however, their applicability to small and semi-enclosed coastal environments such as Harima Nada may be subject to certain limitations. In addition, offline forcing approaches typically rely on prescribed atmospheric conditions and therefore may not fully capture air-sea interactions associated with tidal variability in sea surface height, potentially leading to uncertainties in the simulation of surface conditions in some cases. Coupled atmosphere- ocean modeling frameworks provide an alternative approach for representing these interactions in a more physically consistent manner.

Moreover, as a semi-enclosed and shallow coastal sea with limited exchange with the open ocean, Harima Nada is highly sensitive to riverine runoff [4,10] and atmospheric conditions [11]. Atmospheric conditions, including wind speed and air temperature, govern surface mixing and vertical transport of nutrients [12], further underscoring the importance of coupled atmosphere-ocean interactions. This geographical setting also amplifies the influence of terrestrial inputs, particularly freshwater discharged

from rivers. As a result, river inflows can substantially modify vertical density stratification, mixing intensity, and nutrient transport processes within the system.

Given the considerations outlined above, it is essential to assess the influence of river discharge on the physical environment of Harima Nada before evaluating its nutrient dynamics. In a previous study, a coupled ocean-atmosphere modeling framework was successfully developed for the Seto Inland Sea and applied to investigate the seasonal dynamics of the Kako River discharge into Harima Nada [12]. That study demonstrated the capability of the coupled ROMS-WRF system to represent river-induced circulation features and seasonal variability, establishing a foundation for further applications of coupled modeling approaches in this region. Building upon the previous study, this study extends the coupled modeling framework to explicitly include all major rivers discharging into Harima Nada, with a focus on evaluating the seasonal impacts of river inflow on the physical fields of the coastal sea. This study aims (1) to evaluate the reproducibility of the ocean model under scenarios with and without river inflow using observed hydrographic data, thereby assessing the extent to which river discharge improves model performance; (2) to quantify the seasonal impacts of river inflow on water temperature, salinity, and density structure by comparing simulations with and without river discharge; and (3) to apportion the relative contributions of individual rivers across seasons and to clarify their respective roles in modifying the spatial structure of the physical environment.

Given the ongoing oligotrophication in Harima Nada, quantifying the influence of river inflow on physical fields is a fundamental prerequisite for defining and parameterizing biochemical processes. The process-based physical insights obtained in this study provide essential information for the development of numerical models that simulate nutrient and pollutant cycles, and thereby provide a scientific basis for future evaluations of nutrient management strategies under changing environmental conditions.

2. RESEARCH SIGNIFICANCE

This study underscores the role of river discharge in shaping the physical environment of Harima Nada. By comparing ocean conditions with and without river inflows, the study clarifies how river discharge influences seasonal variations in water stratification and physical characteristics, as well as the extent to which individual river contributes to these changes. Our findings provide a foundation for future biogeochemical modeling in

Harima Nada and support ongoing efforts to develop seasonally adaptive management strategies.

3. METHODOLOGY

3.1 Model Structure

Figure 1 shows an overview of our coupled modeling system. Within this system, meteorological forcing generated by the Weather Research and Forecasting (WRF) model is supplied to the Regional Ocean Modeling System (ROMS) at each calculation step. Using these atmospheric inputs in combination with the Coupled Ocean-Atmospheric Response Experiment bulk flux algorithm [13], ROMS calculates surface momentum and heat fluxes that define the upper boundary conditions of the ocean model. The ROMS-simulated Sea Surface Temperature (SST) is then transferred back to WRF, completing the two-way air-sea coupling. Through this simultaneous two-way exchange of information, the coupled model can reproduce realistic ocean-atmosphere interactions over the Harima Nada region. Compared with one-way atmospheric forcing, the two-way coupled approach explicitly accounts for feedbacks between SST and the atmospheric boundary layer, enabling the representation of short-term ocean-atmosphere interactions. This is particularly important in semi-enclosed coastal seas such as Harima Nada, where air-sea interactions can significantly influence surface stratification and circulation.

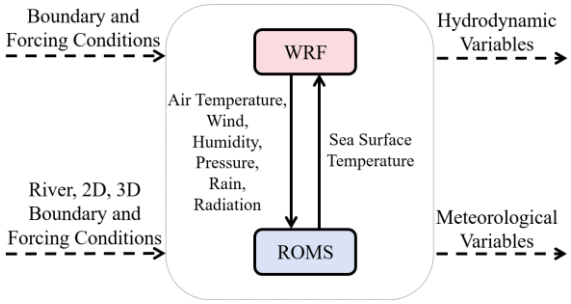

Fig.1 Structure of the ROMS-WRF Coupled Model

3.2 Model Conditions

3.2.1 ROMS and WRF model conditions

The model configuration is summarized in Table 1. The simulation period extends from December 2009 to November 2010, with a six-month spin-up (June - November 2009) to ensure adequate model stability. The simulation period was selected based on both data availability and representativeness of hydrological conditions. Previous studies [14] have demonstrated that river discharge and total nitrogen loads simulated by the applied river model are well reproduced for this period, and that precipitation conditions in 2010 were close to the climatological mean, without pronounced extreme events. This indicates that 2010 represents a climatologically

representative year, suitable for isolating typical seasonal responses of the coastal system under stable forcing conditions. The ROMS computational domain encompasses the entire Seto Inland Sea. Because atmospheric phenomena, including typhoons and heavy rainfall, influence oceanic conditions over large spatial scales, the WRF model domain is designed to encompass western Japan. The atmosphere-ocean exchange between WRF and ROMS is performed at a frequency consistent with the model integration to ensure numerical stability and air-sea interaction. At each coupling step, SST is transferred from ROMS to WRF, while surface momentum, heat, and freshwater fluxes are provided from WRF to ROMS. Air-sea coupling was applied consistently throughout the simulations. Given the extremely shallow bathymetry of the Harima Nada region, the ocean model employs vertically uniform terrain-following layers to maintain numerical stability. In shallow coastal environments, a strongly stretched sigma-coordinate system can produce unduly thin surface layers, potentially compromising numerical stability and solution accuracy. This issue is particularly relevant in regions. Therefore, a vertically uniform layer configuration was adopted to ensure robust model performance. In this study, particular emphasis is placed on evaluating the influence of river discharge on the coastal environment. Accordingly, two river boundary conditions are implemented: simulations without river inflow (w/o) and with river inflow (with) to assess the effects of river discharge on the modeled physical fields.

Table 1. Model configurations applied to the ROMS -WRF coupled model for Harima Nada

ROMS model		
Version		3.9
Horizontal domain		the Seto Inland Sea
Horizontal resolution		3.0 km
Grid size (X Y)		200 × 100
Vertical layer number		32
Time step		60 seconds
Vertical distribution		Equal Layer Thickness
Turbulence model		Mellor-Yamada Level 2.5
Boundary conditions	Ocean	HYCOM-NCODA (1hour, 1/12°)
	Tidal	TPXO9 Atlas v.5
	River	1. without river input 2. with river input
WRF model		
Version		4.2.2
Horizontal domain		the entire western Japan
Horizontal resolution		6.0 km
Vertical layer number		30
Time step		25 seconds
Boundary condition		ERA5
Physics option	microphysics	Morrison 2-moment sheme
	cumulus	no cumulus
	planetary boundary layer	MYNN3
	land-surface	Noah LSM
	radiation	RRTMG

3.2.2 River Boundary Conditions

The river boundary conditions are summarized in Table 2. The model incorporates not only the major rivers that discharge directly into Harima Nada but also key rivers from adjacent coastal regions to more accurately capture the freshwater influence. Both river discharge and river temperature are described with hourly resolution. Figure 2 presents the time series for the total river discharge (11 Harima Nada rivers + 7 rivers from neighboring areas), mean river temperature, and the average sea surface temperature, which is included as a reference following previous studies [15]. Regarding the vertical structure of river inflow, the model uses the layer-wise source option in ROMS, which is widely adopted to ensure numerical stability. This approach avoids the Courant-Friedrichs-Lewy (CFL) instabilities associated with the alternative river runoff method. This configuration allows a stable representation of river forcing without introducing artificial vertical stratification. In addition, the model accounts for the specified depth of each river by distributing freshwater uniformly across the river-affected vertical layers. River discharge and river temperature were prescribed using monthly values, which represent the highest temporal resolution consistently available from publicly accessible river datasets for the study region and are sufficient for the seasonal-scale analysis conducted here.

Regarding the reliability of river discharge estimates, previous evaluations [14] have demonstrated that the Modified Hydro-BEAM model reliably reproduces observed river discharge, supporting the suitability of the applied discharge estimates for this study. River inflow is introduced using a specified river depth and is assumed to be vertically well mixed within that depth. The uniform vertical distribution of river inflow is employed to maintain numerical stability in the shallow coastal environment of Harima Nada. Given the shallow bathymetry and the focus on basin-scale circulation and stratification, this configuration provides a robust and physically consistent representation of river forcing.

Table 2 The river boundary conditions

River boundary conditions	
Number of rivers	18 rivers, 11 that flow directly into Harima Nada 7 from neighboring coastal regions (Osaka Bay, Kii Channel and Bisan Strait)
River discharge	Results from Modified Hydro–BEAM [14] and Water Information System [16]
River temperature	Monthly water temperature values of each river [16]
PSU	0
River vertical distribution	Perfectly mixed river inflow; uniform vertical distribution within the river depth

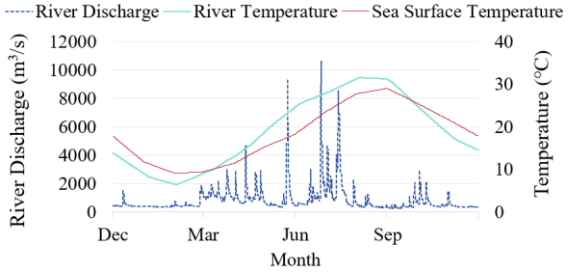

Fig.2 Time series of river discharge, river temperature and sea surface temperature of the study area

3.3 Study Area and Evaluation Method

As shown in Figure 3, the study area covers the entire Harima Nada. Model reproducibility under the with and without river inflow conditions was evaluated using temperature and salinity observations from 15 observation points [17]. Observed and simulated values were compared at three depths (0.5 m at the surface, 10 m at mid-depth, and 1 m above the sea bottom) over the full simulation period (winter: December – February; spring: March – May; summer: June – August; fall: September – November).

To further evaluate the effects of river discharge, seasonal mean vertical profiles of temperature, salinity, and density from the 15 points were compared between with and without river inflow calculations. This seasonal analysis clarifies how river discharge modifies the vertical structure of the water column throughout the year.

To assess the contribution of individual rivers, tracer-based diagnostics were applied at the same 15 points. One tracer was assigned to each river and scaled to its discharge. Table 3 summarizes the modeled estuary locations and the annual average discharge for each river. The resulting seasonal fractions were used to evaluate the relative influence of individual rivers on the system.

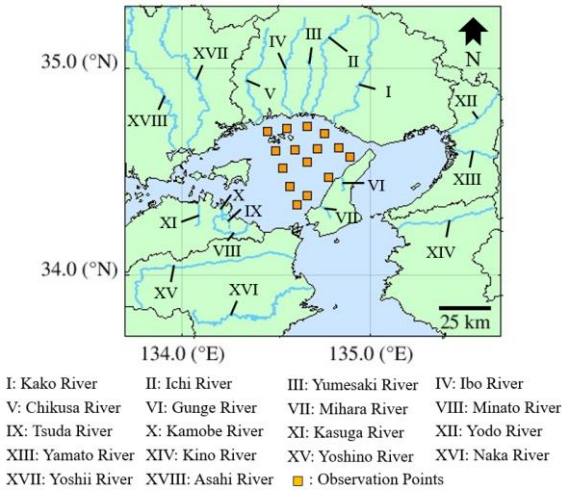

Fig.3 The study area

Table 3 Modeled river estuary locations and annual average discharge

River	Latitude (°N)	Longitude (°E)	River discharge (m^3/s)
Kako	34.695	134.769	71.28
Ichi	34.722	134.688	25.57
Yumesaki	34.722	134.661	9.16
Ibo	34.722	134.580	38.52
Chikusa	34.695	134.391	28.86
Gunge	34.533	134.823	0.58
Mihara	34.371	134.688	7.26
Tsuda	34.317	134.364	1.27
Kamobe	34.290	134.283	2.04
Minato	34.398	134.202	1.83
Kasuga	34.425	134.067	5.61
Yodo	34.641	135.363	221.46
Yamato	34.560	135.363	27.28
Kino	34.182	135.093	50.59
Yoshino	34.128	134.661	182.77
Naka	33.966	134.769	65.70
Yoshii	34.560	134.121	56.18
Asahi	34.560	134.094	42.55

4. RESULTS AND DISCUSSION

4.1 Reproducibility

4.1.1 Sea Water Temperature

Table 4 compares the reproducibility of water temperature with and without river inflow. The statistical evaluation indicates a consistent improvement in temperature accuracy when river inflow is included, with the most pronounced enhancement occurring in summer and fall. This improvement reflects the influence of river inflow through freshwater-induced stratification and its modulation of vertical mixing, rather than a simple warming effect. In contrast, the river influence is weaker in winter and spring, when temperature variability is mainly controlled by strong vertical mixing and atmospheric heating. Although the baseline simulation already reproduces seasonal temperature reasonably well, river inflow provides additional refinement during periods of strong stratification and seasonal transition. This behavior is also evident in Figure 4, which shows the mean temperature at the 15 observation points and a similar temporal pattern.

Table 4 Reproducibility metrics for simulated water temperature

	River	R	MBE	RMSE	IA
Annual	w/o	0.99	-0.69	1.23	0.99
	with	0.99	-0.57	1.10	0.99
Winter	w/o	0.99	-0.05	0.54	0.99
	with	1.00	-0.01	0.51	0.99
Spring	w/o	0.95	-0.03	0.73	0.97
	with	0.95	-0.04	0.78	0.96
Summer	w/o	0.96	-1.22	1.67	0.95
	with	0.96	-1.13	1.53	0.96
Fall	w/o	0.98	-1.44	1.57	0.91
	with	0.98	-1.10	1.29	0.93

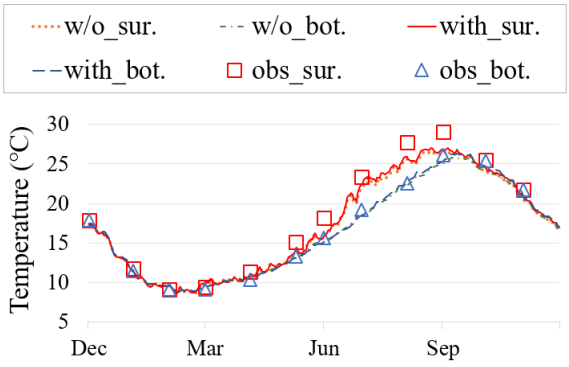

Fig.4 Time series of sea water temperature averaged over the 15 observation points

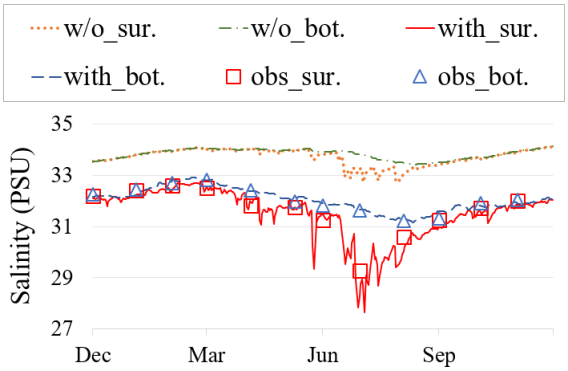

Fig.5 Time series of sea water salinity averaged over the 15 observation points

4.1.2 Sea Water Salinity

As shown in Table 5, the accuracy of simulated salinity improves markedly under the river inflow condition. The mean bias error (MBE) remains within 0.13 PSU across all seasons, indicating that the spatial distribution of salinity in Harima Nada is well reproduced. In winter, although the RMSE is reduced by correcting the overall salinity bias, the correlation coefficient (R) decreases slightly. This reflects the relatively small seasonal variability of salinity during winter, under which R becomes more sensitive to minor timing differences and short-term fluctuations. Overall, the combined evaluation metrics confirm an improved representation of winter salinity under the river inflow condition.

Figure 5 presents the mean values averaged over all observation points. The results show that simulations considering river inflow reproduce the observed seasonal variations, demonstrating the substantial role of freshwater input in shaping the salinity field across the region. The model performance exhibits consistent improvement in both coastal and offshore areas, indicating a system-wide response rather than a localized coastal effect. This widespread enhancement reflects the characteristic geometry of Harima Nada as a semi-enclosed and relatively shallow basin, which facilitates the efficient propagation of river-derived freshwater signals and allows variations in river discharge to influence offshore areas to a comparable extent.

Table 5 Reproducibility metrics for simulated water salinity

	River	R	MBE	RMSE	IA
Annual	w/o	0.64	1.90	2.01	0.36
	with	0.90	-0.07	0.42	0.94
Winter	w/o	0.79	1.33	1.34	0.23
	with	0.66	-0.13	0.31	0.72
Spring	w/o	0.23	1.77	1.84	0.23
	with	0.80	0.03	0.32	0.89
Summer	w/o	0.61	2.52	2.64	0.31
	with	0.88	-0.08	0.61	0.92
Fall	w/o	0.79	1.98	2.00	0.27
	with	0.74	-0.10	0.35	0.83

4.2 Vertical Differences in Physical Fields

4.2.1 Sea Water Temperature

Figure 6 shows the vertical differences in mean temperature across all observation sites in Harima Nada, calculated as the mean temperature with river inflow minus the mean temperature without river inflow.

During winter, the inflow of cold river water lowers sea surface temperature, weakening density stratification and enhancing vertical mixing. Under these conditions, the water column is weakly stratified and highly responsive to external freshwater perturbations. This deeper mixing allows relatively warmer mid-layer water to be transported downwards and to replace the colder bottom water, resulting in an increase in bottom temperature despite surface cooling. As solar heating intensifies in spring and stratification begins to re-establish, it limits the influence of freshwater on the thermal structure. During this transitional period, atmospheric heat flux becomes the primary control on surface temperature evolution. Although the slightly warmer river inflow leads to minor surface warming, the reduced vertical exchange prevents heat from penetrating to depth, resulting in weakly warming waters at the surface and slightly cooling ones at the bottom. With the onset of summer, substantially warmer river inflows and increased discharges, temperatures rise throughout the water column, and density stratification strengthens and deepens, resulting in the largest temperature gradient between surface and bottom. The strong density contrast effectively suppresses vertical mixing, allowing surface warming to persist while isolating the bottom layer. By early fall, river water remains warmer than the surrounding seawater, and residual summer heat maintains elevated temperatures throughout the column. This reflects the persistence of summer thermal memory within the water column. As seasonal cooling progresses and stratification weakens, the temperature increase becomes more uniformly distributed rather than being confined to surface layers.

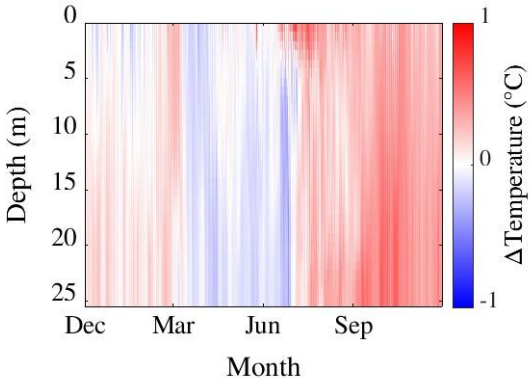

Fig.6 Time series of full depth temperature differences (with river inflow – without river inflow), averaged over the 15 observation points

4.2.2 Sea Water Salinity

Figure 7 shows the annual salinity differences. The figure indicates that the values are lower across the entire water column throughout the year in the simulation incorporating river discharge. The salinity reduction is directly associated with riverine freshwater input and seasonal stratification.

The seasonal response of salinity shows clear contrasts throughout the year. During winter, freshwater input is minimal, and the resulting salinity difference remains below 1 PSU, indicating a weak influence on the water column. As solar heating increases in spring, density stratification strengthens, limiting vertical mixing and producing a more pronounced surface reduction. With the onset of summer, intensified river discharge and stratification result in an average salinity reduction of ~5 PSU in the upper layer (surface to ~5 m). Despite the strongly layered structure, this season exhibits the largest reduction across the entire water column. As conditions transition into fall, increasing vertical mixing weakens stratification, yielding a more uniform decrease in salinity with depth.

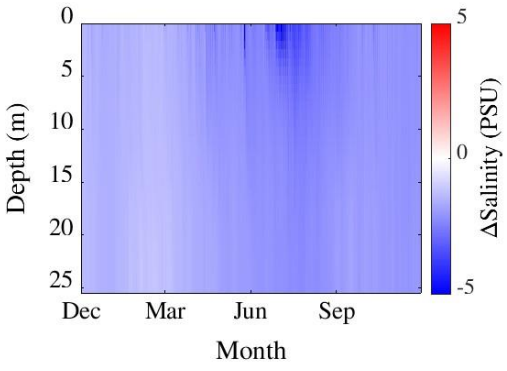

Fig.7 Time series of full depth salinity differences (with river inflow – without river inflow), averaged over the 15 observation points

4.2.3 Sea Water Density

Seawater density is primarily governed by temperature and salinity, and a pronounced vertical density gradient between the surface and bottom layers indicates strong stratification. Such stratification suppresses vertical mixing and influences the distribution and transport of freshwater within the coastal system. Seawater density increases with decreasing temperature and increasing salinity. Consequently, river inflow introduces relatively warm and low-salinity freshwater to the coastal zone, producing a buoyant surface layer. This buoyancy input modifies the vertical density stratification and subsequently influences the degree of mixing between the upper and lower water columns.

Furthermore, to quantify the strength of density lamination, the Brunt - Väisälä oscillation frequency (N^2) is often used as a measure of the vertical stability of the water column. N^2 is defined as [18]:

$$N^2 = -\frac{g}{\rho_0} \cdot \frac{d\rho}{dz} \quad (1)$$

Where g is gravitational acceleration (m/s²), ρ_0 is reference density (kg/m³), and $d\rho/dz$ is the vertical gradient of density (kg/m⁴). The larger the N^2, the more stable the stratification of the water column is, and the more difficult the mixing between layers. This indicator can effectively reflect the combined effects of temperature and salinity changes on the density structure.

Figure 8 shows the time-series variation of N^2 in the annual season (with and without river inflow conditions). Values around 0 indicate a more unstable water column, whereas values close to 1 indicate a stable condition. The figure shows that, in the absence of river discharge, the water column remains largely unstable throughout the year except in summer months, when atmospheric freshwater input and surface heating lead to a relatively stabilized upper layer. In contrast, when river inflow is included, the water column becomes slightly more stable even during the cold winter months due to the buoyancy contribution of freshwater. From late spring to summer, pronounced stratification develops, and a highly stable structure is maintained from the surface to approximately 10 m depth. During this period, the relative importance of buoyancy forcing increases as vertical mixing weakens. This seasonal transition marks a shift from a mixing-dominated regime to a buoyancy-controlled stratified regime, in which atmospheric surface heating initiates stratification and freshwater input acts to reinforce water-column stability by limiting vertical exchange. This enhanced stability therefore arises primarily from seasonal surface warming, with additional amplification from the influx of warm, low-salinity river water; this freshwater input increases upper-layer buoyancy, steepens the density gradient between the surface and bottom layers, and thereby suppresses vertical mixing.

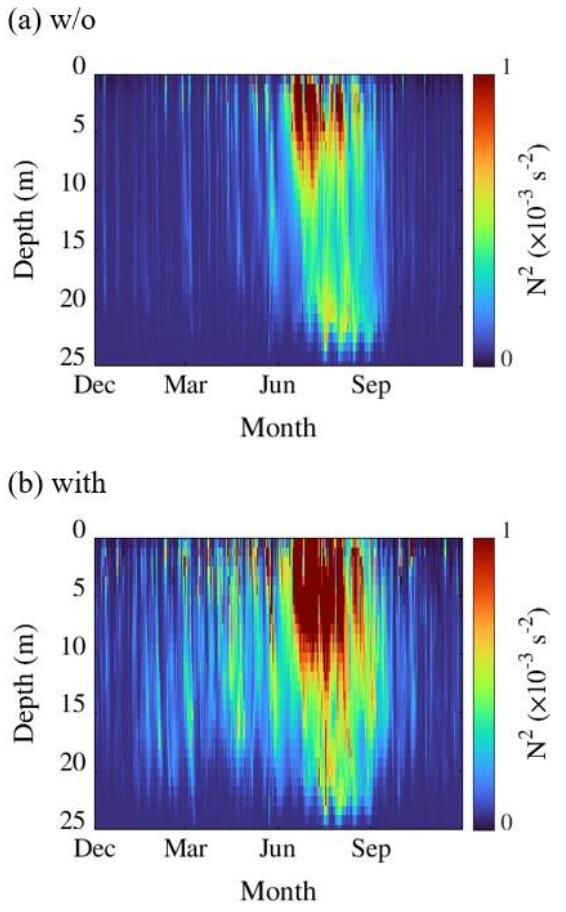

Fig.8 Time series of variation of Brunt - Väisälä frequency squared (N^2), averaged over the 15 observation points

4.3 Relative Contributions of Rivers Discharging into Harima Nada

Table 6 summarizes the relative contribution of individual rivers to the total freshwater input into Harima Nada on both an annual and seasonal basis. The table indicates that the seasonal contributions of individual rivers do not differ substantially from their annual proportions, because the relative discharge hierarchy among the rivers is largely maintained throughout the year despite seasonal fluctuations in absolute flow. Among them, the river exerting the greatest influence is the Yodo River, which discharges directly into Osaka Bay. Its contribution reaches up to 25% in fall, with an annual mean of 22%. This relatively high contribution is attributable to the large annual mean discharge (shown in Table 3) of the Yodo River. Although it does not flow directly into Harima Nada, the discharge-driven circulation facilitates the transport of freshwater towards Harima Nada. The second-largest contributor is the Kako River, accounting for 16% of the annual proportion. This is because, among the rivers that discharge directly into Harima Nada, it has the highest annual mean discharge, and its inflow enters the basin without significant dilution, thereby exerting a substantial influence on the total freshwater input.

In addition, the Ibo River and the Chikusa River (in the northern part of Harima Nada), as well as the Yoshii River and Asahi River (discharging into the adjacent Bisan Strait), also contribute substantially and should not be overlooked. Their comparatively larger discharge volumes, together with their geographical proximity to the northern opening of the basin, enable their freshwater input to be more effectively conveyed into Harima Nada, resulting in a clearer contribution relative to other sources. In contrast, the rivers entering from the southern sector of Harima Nada, together with the Yoshino and Naka Rivers flowing into the Kii Channel, exhibit very small contributions. Their limited discharge and indirect connection result in only a minor contribution compared with the northern rivers.

Table 6 Relative contributions of rivers discharging into Harima Nada

River	Annual	Winter	Spring	Summer	Fall
Kako	16	16	18	16	15
Ichi	6	7	7	7	6
Yumesaki	2	2	2	2	2
Ibo	10	13	11	9	10
Chikusa	7	10	7	6	7
Gunge	*	*	*	*	*
Mihara	1	1	1	1	1
Tsuda	*	1	*	*	*
Kamobe	1	1	1	1	*
Minato	1	1	1	1	*
Kasuga	1	2	1	1	1
Yodo	22	14	22	24	25
Yamato	3	3	3	3	3
Kino	3	2	3	3	3
Yoshino	7	7	6	7	7
Naka	1	*	*	1	2
Yoshii	11	12	10	10	10
Asahi	8	8	7	8	8

*: contribution is not significant for the entire area analysis

To further analyze the vertical distribution of the river-derived water fraction from the major contributing rivers across Harima Nada throughout the year, Figure 9 presents the spatial patterns for the Kako River and the Yodo River. In the case of the Kako River, surface concentrations are elevated, with markedly lower values at depth, highlighting the presence of strong density stratification. This is attributable to its direct inflow into Harima Nada, which delivers freshwater at the surface and therefore produces a surface-intensified tracer signal. Because the buoyant river plume remains confined to the upper layer and experiences limited vertical mixing, the tracer is rapidly advected horizontally rather than being transported downward, resulting in a distinct vertical gradient.

In contrast, the freshwater associated with the Yodo River is vertically uniform in Harima Nada. This vertical uniformity forms because the water is

already mixed upstream before entering Harima Nada. After the Yodo River water enters Osaka Bay, it is carried toward the Akashi Strait, where strong vertical mixing further homogenizes the water column. Previous studies have also documented vigorous mixing in this strait [19]. Moreover, the enhanced momentum associated with the larger inflow promotes stronger vertical mixing and downward penetration of river-derived water. As a result, the freshwater signal is not confined to the surface layer but redistributed through active exchange. These processes influenced the spatial signal of the Yodo River, allowing it to extend beyond the near-surface region and spread laterally. Consequently, the Yodo River signal in Harima Nada reflects basin-scale dilution and efficient vertical exchange, rather than a surface-intensified plume shaped by momentum-driven mixing.

The physical framework established in this study represents a first step toward developing a regional biogeochemical model that provides the necessary physical basis for evaluating management strategies to address oligotrophication and for examining system responses under future scenarios.

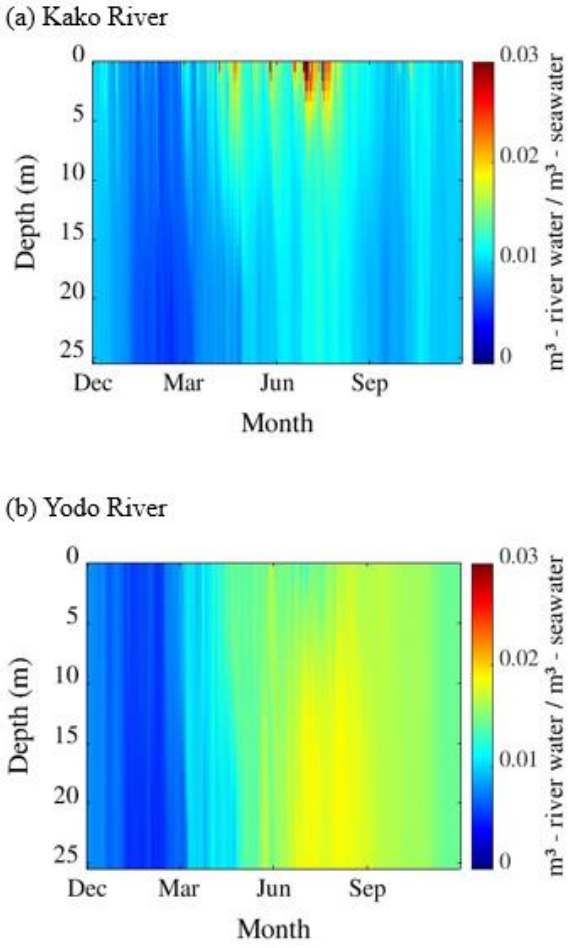

Fig.9 Time series of river inflow water fraction in seawater, averaged over the 15 observation points

5. CONCLUSIONS

In this study, a coupled ocean–atmosphere modeling system was applied to quantify the influence of river discharge on the physical environment of Harima Nada. By comparing simulations with and without river inflow, the model's performance in reproducing the regional hydrodynamics was assessed, and the annual and seasonal spatial differences in the physical fields were examined to clarify the impacts of river input. In addition, the relative contributions of individual rivers were quantified to determine the extent to which each river affects the physical conditions within Harima Nada.

The results indicate an overall improvement in the model's ability to reproduce temperature and salinity, with a particularly notable enhancement in salinity when river inflow is included. Specifically, the inclusion of river inflow reduced the annual salinity RMSE from 2.01 PSU to 0.42 PSU and increased the index of agreement (IA) from 0.36 to 0.94. The improvement is comparable between the coastal and offshore regions, demonstrating a basin-wide response. This is attributed to the semi-enclosed and relatively shallow bathymetry of Harima Nada, which makes the system highly sensitive to river discharge.

Regarding the spatial distribution of the physical fields, although river inflow does not substantially improve model performance for water temperature, the seasonal statistics exhibit differences when both conditions are compared. In the case of salinity and water column stability, results effectively captured the natural seasonal influence of freshwater input. The salinity fields exhibit pronounced freshening during periods of increased river discharge, while the stability index shows a corresponding enhancement of stratification in the upper layer. These seasonal responses indicate that freshwater input not only modifies the horizontal distribution of salinity but also regulates the vertical density structure, resulting in enhanced stratification during warmer months and weakened water-column stability during periods of low discharge.

The analysis of the relative influence of individual rivers further demonstrates that, among these rivers, the Yodo and Kako rivers make the largest contributions, accounting for 22% and 16% of the total freshwater input, respectively, and that tracers originating from major rivers discharging into neighboring regions such as the Bisan Strait, the Kii Channel, and Osaka Bay exert a contribution to Harima Nada that is comparable to the smaller rivers entering from the northern side of the basin. These inputs represent a non-negligible source of freshwater influence and need to be considered when evaluating the hydrographic conditions of Harima Nada, rather than being treated as externally isolated or insignificant. Their detectable contribution also

indicates that the basin is not solely affected by direct local inflow, but is influenced by broader regional connectivity. In contrast, the impact of the small to medium-sized rivers that discharge directly into the central and southern sectors of Harima Nada, as well as those discharging in the Kii Channel area, is limited. Their contributions remain minor due to their relatively low discharge volumes and the geographical disconnection of the Yoshino River, despite its comparatively large, resulting in only a weak tracer signal. Consequently, their influence on the overall freshwater characteristics of Harima Nada is largely confined to very shallow coastal areas near their estuaries, while remaining relatively small compared with that of the northern rivers and major rivers from adjacent regions. In contrast, although the Yoshino River supplies a much larger freshwater volume, its geographically distant estuary and flow pathway prevent its tracer signal from reaching Harima Nada in any appreciable way.

Overall, this study establishes a physically consistent foundation that supports future efforts to integrate biogeochemical processes at the regional scale. By providing a reliable representation of the physical environment, the present framework provides a robust foundation for evaluating management strategies addressing oligotrophication and for exploring potential system responses under future scenarios.

6. REFERENCES

1. Yamamoto T., Oligotrophication of the Seto Inland Sea - Revisited. Journal of the JIME, Vol. 49, No. 4, 2014, pp. 496-501. https://doi.org/10.5988/jime.49.496
2. Yamamoto, Tamiji. The seto Inland sea—eutrophic or oligotrophic?. Marine Pollution Bulletin, 47. 1-6, 2003, pp. 37-42, https://doi.org/10.1016/S0025-326X(02)00416-2
3. Tetsuo Y, Origins of Phosphorus and Nitrogen in the Seto Inland Sea, Japan, Research Institute for Applied Mechanics, Kyushu University, 144, 2013, pp. 13-18, https://doi.org/10.15017/27156
4. Abo, K., & Yamamoto, T. Oligotrophication and its measures in the Seto Inland Sea, Japan. Bulletin of the Japanese Fisheries Research and Education Agency, 49, 2019, pp. 21-26
5. Asahi, T.; Ichimi, K.; Yamaguchi, H.; Tada, K. Horizontal distribution of particulate matter and its characterization using phosphorus as an indicator in surface coastal water, Harima-Nada, the Seto Inland Sea, Japan. J. Oceanogr. 2014, 70, pp. 277–287. https://doi.org/10.1007/s10872-014-0230-z
6. Kobayashi, S.; Nakada, S.; Futamura, A.; Nagamoto, K.; Fujiwara, T. Observation and modeling of seawater exchange in a strait-basin system in the Seto Inland Sea, Japan. J. Water Environ. Technol. 2019, 17, pp. 141–152. https://doi.org/10.2965/jwet.18-042
7. Uchiyama Y., Ishii S. and Miyazawa Y., Oceanic Downscaling Effects on the Kuroshio Extension Jet using a JCOPE2-ROMS System, J.JSCE, Ser.B2, Coastal engineering, Vol. 68，No. 2，2012 , pp. 436-440. https://doi.org/10.2208/kaigan.68.I_436
8. Tanaka Y., Mori N., Ninomiya J., Sugimatsu K., Yagi H., Yasuda T. and Mase H., Long and Short-Term Simulations of Seto Inland Sea by Coupled Ocean-Wave Model, J.JSCE, Ser.B2, Coastal engineering, Vol. 69，No. 2，2013，pp. 511-515. https://doi.org/10.2208/kaigan.69.I_511
9. Yoshie N., Current Status and Problems of the End-to-End Model Including Processes from Nutrient Cycles to a Higher-Trophic-Level Marine Ecosystem, Bulletin on coastal oceanography, Vol.60, No.1, 2022, pp. 41-50, https://doi.org/10.32142/engankaiyo.2022.8.002
10. Abo, K.; Satoshi, A.; Kazuhiro, H.; Yoshiki, N.; Hayashi, H.; Murata, K.; Wanishi, A.; Ishikawa, Y.; Masui, T.; Nishikawa, S.; et al. Long-Term Variations in Water Quality and Causal Factors in the Seto Inland Sea, Japan. Bull. Coast. Oceanography, 55, 2018, pp. 2101–2111, https://doi.org/10.32142/engankaiyo.55.2_101
11. Abo, K., Akiyama S., Harada K., Nakaji Y., Hayashi H., Murata K., Wanishi A., Ishikawa Y., Masui T., Nishikawa S., Yamada K., Noda M and Tokumitsu S., Long-Term Variations in Water Quality and Causal Factors in the Seto Inland Sea, Japan. Bulletin on Coastal Oceanography, Vol.55, No.2, 2018, pp.101-111, https://doi.org/10.32142/engankaiyo.55.2_101
12. PINTOS ANDREOLI Valentina, Shimadera H., Yasuga H., Koga Y., Suzuki M., and Kondo A., Seasonal Study of the Kako River Discharge Dynamics into Harima Nada Using a Coupled Atmospheric-Marine Model, Water, Vol. 16, 614, 2024, https://doi.org/10.3390/w16040614
13. John C. Warner., Brandy Armstrong., Ruoying He and Joseph B. Zambon., Development of a Coupled Ocean-Atmosphere-Wave–Sediment Transport (COAWST) Modeling System, Ocean Modelling 35, 2010, pp. 230-244, https://doi.org/10.1016/j.ocemod.2010.07.010
14. V Pintos Andreoli, M Mori, Y Koga, H Shimadera, M Suzuki, T Matsuo and A Kondo, Numerical Assessment of Total Nitrogen (Tn) Load Discharged from Rivers into Harima-Nada, the Seto Inland Sea, Using A Numerical Coupled Hydrological-Water Quality Model. IOP Conference Series: Earth and Environmental Science, 801, 012009, 2021, DOI :10.1088/1755-1315/801/1/012009
15. Takakura R., Miyahara K. and Miyada K., Comparing Statistical Evaluations of Water Temperature in Harima Nada, Hyogo Prefecture,

Bulletin of the Hyogo Prefectural Technology Center for Agriculture, Forestry and Fisheries, 3:8-17, 2020, pp. 8-17
16. Ministry of Land, Infrastructure, Transport and Tourism, Water Information System
17. Hyogo Prefectural Technology Center for Agriculture, Forestry and Fishery. Harima Nada Observatories. Available online: https://www.hyogo-suigi.jp/gj/
18. Brassard, P., Fontaine, G., Wesemael, F., Kawaler, S. D., & Tassoul, M., Adiabatic properties of pulsating DA white dwarfs. I - The treatment of the Brunt-Vaisala frequency and the region of period formation, Astrophysical Journal, Part 1 (ISSN 0004-637X), vol. 367, Feb. 1, 1991, pp. 601-611
19. Fujiwara T., Kobayashi S., Kunii M. and Uno N., Field observations of nitrogen and phosphorus transport and sources in the Seto Inland Sea [in Japanese]. Proceedings of Coastal Engineering, JSCE, 50, 2003, pp, 951-955, https://doi.org/10.2208/proce1989.50.951